IEEE Access
Multidisciplinary | Rapid Review | Open Access Journal

IEEE VEHICULAR TECHNOLOGY SOCIETY SECTION

Received November 17, 2021, accepted December 14, 2021, date of publication December 16, 2021,
date of current version December 27, 2021.

Digital Object Identifier 10.1109/ACCESS.2021.3136129

An SDN/ML-Based Adaptive Cell Selection Approach for HetNets: A Real-World Case Study in London, UK

IBTIHAL AHMED ALABLANI[1,2] AND MOHAMMED AMER ARAFAH[1]

[1]Department of Computer Engineering, College of Computer and Information Sciences, King Saud University, Riyadh 11543, Saudi Arabia
[2]Department of Computer Technology, Technical College, Technical and Vocational Training Corporation, Riyadh 11472, Saudi Arabia

Corresponding author: Ibtihal Ahmed Alablani (438203904@student.ksu.edu.sa)

This work was supported by the Research Group of the Deanship of Scientific Research at King Saud University under Grant RG-1440-122.

ABSTRACT Heterogeneous networks (HetNets) are one of the key enabling technologies for next-generation networks. They aim to provide high capacity, low installation cost, and distributed traffic loads. The cell selection issue is an open research problem in HetNets, due to the different characteristics of base stations and the existence of a large number of them. In this paper, a novel software-defined networking (SDN)/machine learning (ML)-based adaptive algorithm is proposed, called adaptive two-tier, based on the K-nearest neighbor (A2T-KNN) algorithm. It is designed for millimeter wave (mmWave)-based HetNets and it has the ability to adapt to the various movement features of moving vehicles, as well as the different characteristics of the base stations. A real-world case is considered in the center of London. Simulation results demonstrate that A2T-KNN achieves high prediction performance in association with different vehicle features and configuration information. It outperforms other related schemes in terms of average number of handovers by up to 45.83%. Moreover, it was found to enhance the average achievable downlink data rate and network energy efficiency achieved by vehicles by up to 17.18% and 16.86%, respectively.

INDEX TERMS 5G, small cells, SDN, London, machine learning, HetNets, adaptive selection.

I. INTRODUCTION

London is the capital city of the United Kingdom (UK) [1]. It has a geographical area of 607 square kilometers and it is the most densely populated city of the UK. In 2016, the population density per square kilometer was 5590. To make London a smart city, the Smart London Board was established to transform the traditional systems of energy, healthcare, pollution management, transport, and traffic into smart services [2], as figure 1 shows. By 2036, London will become a mega-smart city with 10 million citizens [3].

Smart city refers to a modern city that employs advanced technologies to enhance the lives of its residents [4]. Wireless cellular networks are a fundamental component of smart cities [5]. They are used to enable numerous applications and services, such as the Internet of Things (IoT), virtual reality, and many more. [6]–[8]. Future wireless networks are projected to apply heterogeneous networks enabling technology to fulfill the different requirements of user equipment [9]. HetNets are networks that have a mix of conventional high-power macro and low-power small base stations (BSs) [10]. Small BSs are deployed in HetNets to improve capacity and to distribute traffic loads with a low installation cost [11], [12]. Figure 2 represents a map of London, showing the locations of the macro and small BSs operated by Vodafone. As shown in the figure, there is a high density of small BSs in the middle of London.

Cell selection refers to the process of choosing a serving BS based on certain criteria. However, the cell selection issue in 5G HetNets is a challenging task that affects the performance of users and the network due to different cell sizes, as well as high spectrum reuse [13], [14]. In addition, the movement of vehicles in the small coverage area of the small BSs leads to increasing handover (HO) rates [15]. Handover procedure includes three phases; preparation, execution and completion [16]. Figure 3 displays the HO phases, showing the signaling overhead during these phases. In the preparation phase, a vehicle measures the radio resource

The associate editor coordinating the review of this manuscript and approving it for publication was Jie Gao.

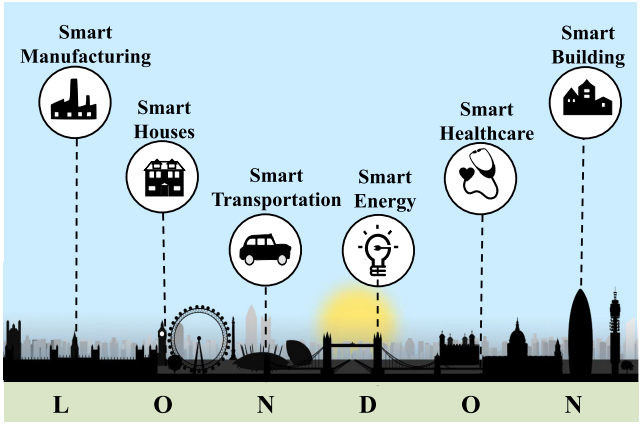

FIGURE 1. The smart city of London.

management (RRM) parameters and then transmits a measurement report to the source BS which decides whether to perform an HO or not. Then, the source BS sends an HO request to one or more target BSs. These BSs perform admission control and they transmit an HO response to the source BS if they can provide the requested resources. At the end of this phase, the source BS selects the best target BS based on the received HO responses. In the execution phase, the source BS sends an HO command to the vehicle to connect to the selected target BS. When the vehicle associates with the target BS, it sends an HO confirmation to the target BS to finish the execution phase. In the completion phase, the target BS informs the core control plane (C-plane) functions to switch path from the source BS to the target BS by transmitting a path switch request. Then, when the path switch response is received by the target BS, it sends a release resource message to the source BS to complete the handover process [17], [18].

Cell selection schemes vary in term of selection method, network modeling, and problem solving, as shown in figure 4. They are classified based on the selection method into static and dynamic. Static selection refers to choosing the serving base station depending on a fixed method based on one criterion or multiple criteria. Dynamic selection, which is also called adaptive selection, means that the method of choosing a serving cell varies based on predefined values [12]. The dynamic method can be applied to single-tier or multi-tier networks. Wireless networks can be modeled based on hypothetical-based (such as hexagonal grid and random distribution) or real-world-based approaches. Solving the cell selection issue can be achieved by applying machine learning techniques or other approaches. Machine learning is a powerful tool that is based on different algorithms to give computer systems the ability to learn from data without programming them explicitly [19]. Nowadays, machine learning techniques have proven to be effective in many prediction tasks [20]. Software-defined networking is one of the most recent network architectures that aims to facilitate the network management task and to enhance the utilization of network resources in an efficient way [21]. The cell selection decision can be centrally coordinated by using an SDN controller [22], and the combination of SDN and ML creates a new network management solution [23]. Applying the traditional scheme that considers the static method with only a single criterion, the Received Signal Strength Indicator (RSSI), in 5G cellular networks is not appropriate due to the existence of a high density of BSs [24], [25]; this will lead to increasing handover rates and service interruptions with unbalanced loads [12], [26]. Most of the existing works use static methods to select the base station to be associated with [12]. There is a need for an adaptive cell selection scheme that can select the best base station by considering the HetNet's features and user equipment (UE) movement information. In addition, most recent works are based on single-tier selection of base stations. In fact, it is necessary to consider multi-tier, where the macro BS tier is still essential to serve high mobility UEs in order to decrease the handover rate [27]. Moreover, applying a certain cell selection strategy to a real-world case is preferable to study the effectiveness of the proposed algorithm in a realistic environment.

In this paper, the major contributions are as follows:

1) We study the cell selection problem of heterogeneous ultra-dense networks by using supervised learning technology. We propose a novel SDN/ML-based adaptive algorithm called A2T-KNN. It aims to intelligently choose the best BS from the two-tier BSs based on vehicle information and the features of the HetNet.
2) We model the heterogeneous ultra-dense networks based on a real-world dataset that was collected in the UK. The macro and small BSs that are operated by Vodafone and located in the central area of London are selected to be the system model.
3) We generate a new vehicle dataset based on London street-related information, using Google Maps and MATLAB 2021a. It includes 38,441 rows and it is used to train and test the used ML models.
4) We perform simulations to evaluate the performance of the proposed A2T-KNN algorithm. The results demonstrate that the proposed algorithm outperforms other schemes in terms of average (a) number of handovers (HOs), (b) staying time, (c) number of HO failures and unnecessary HOs, (d) downlink sum-rate, (e) energy efficiency, (f) radio link failures (RLFs), and (g) handover interruption time (HIT). In addition, the A2T-KNN achieves high accuracy, sensitivity, specificity and precision.

The rest of this paper is organized as follows: Section II provides a review of related works. The proposed scheme and system model are described in detail in Sections III and IV, respectively. Section V presents a performance analysis of the proposed A2T-KNN algorithm. The paper is concluded in Section VI. Appendix provides lists of the main abbreviation and symbols that are mentioned in this paper.

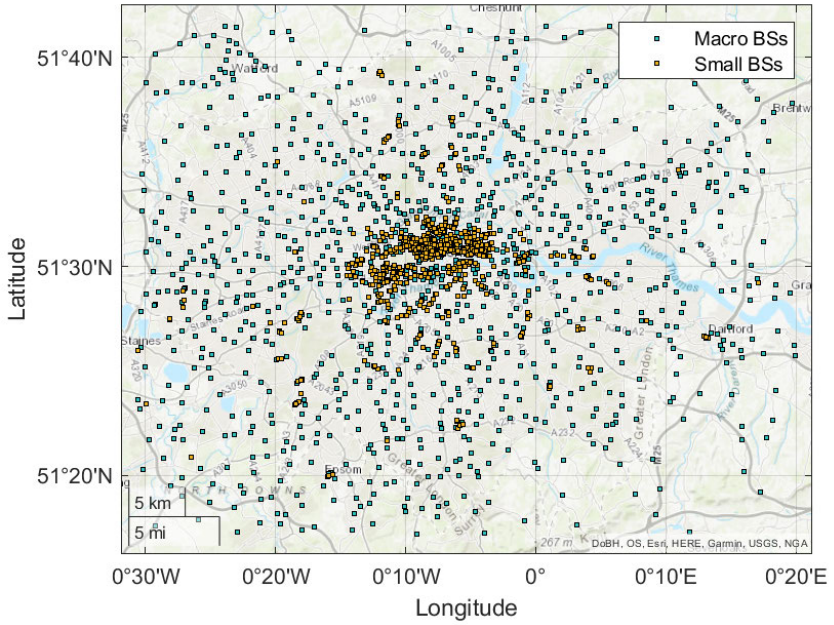

FIGURE 2. London map, showing the base stations operated by Vodafone.

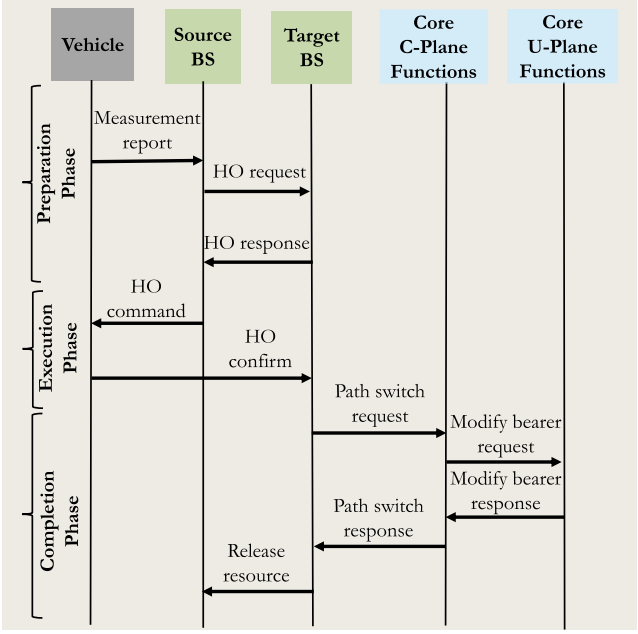

FIGURE 3. The phases of the handover procedure, showing the signaling overhead.

II. RELATED WORK

In [28], Arshad, *et al.* introduced topology-aware skipping schemes by studying the negative impact of user speed on the achieved throughput in ultra-dense networks. The user location and/or cell size are considered when taking the handover decision. Simulation results show that the proposed schemes are superior to the traditional scheme in terms of the average achievable user throughput by up to 47%.

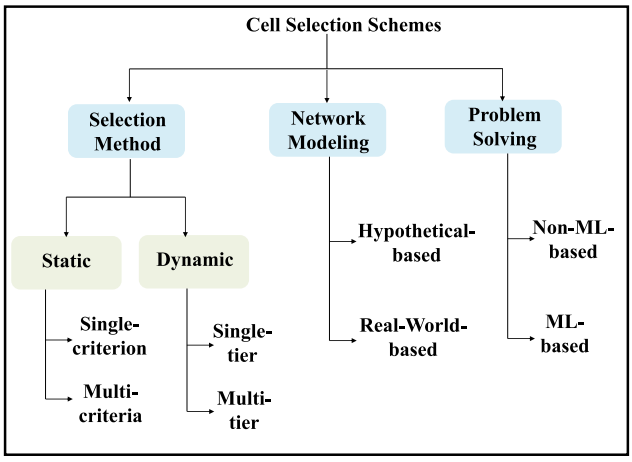

FIGURE 4. Classification of cell selection schemes.

In [29], Tesema *et al.* developed a fast cell selection (FCS) approach for 5G ultra-dense networks to select serving cells from a set called Active Set (AS). To improve the reliability of the communication system, multi-connectivity was considered. The serving base station was selected based on the signal-to-interference-plus-noise ratio value. The study considered both fast and slow user equipment. Simulation results demonstrated that the proposed approach could overcome the problem of radio link failures. Moreover, the achievable throughput was enhanced in comparison with other single-connectivity strategies.

In [30], Cacciapuoti proposed a mobility-aware cell selection scheme for millimeter-wave networks. The proposed

scheme considered the distribution of the loads among the small cells to avoid cell congestion. It reduced the number of frequent handovers between small cells and took into consideration the problems of non-line-of-sight propagation effects, blockage, and directionality. In addition, it could handle changes in the network topology and channel conditions. A polynomial-time complexity figure algorithm was designed to solve the user association issue. The numerical results showed that the proposed scheme outperformed the traditional RSS-based approach.

Wickramasuriya *et al.* proposed a cell selection algorithm for 5G cellular networks in [31]. A Recurrent Neural Network (RNN) was used to predict the optimal BS that a mobile user would be associated with. To train the proposed RNN model, received signal strength (RSS) values were used. The proposed RNN architecture has three layers; input, hidden, and output. The RNN model has 640 neurons and the activation functions used are sigmoid and tanh. To evaluate the performance of the proposed approach, Google's Python-based Tensorflow library was utilized. The learning rate was set to 0.0003 and the model training took 35 minutes. An area of 36 km^2 was considered, with eight base stations distributed randomly. A mobile node, which can be a pedestrian or a vehicle, can connect with the three nearest base stations. Simulation results show that the proposed algorithm achieved 98% accuracy in predicting the next BS.

In [32], Kishida *et al.* proposed a cell selection scheme for 5G multi-tier Radio Access Networks (RANs). The selected cell is the cell that has the maximum signal-to-interference-plus-noise ratio (SINR) value and is located in the user's direction. Real locations of base stations are considered in a metropolitan environment in Shinjuku, Tokyo. Two kinds of users are considered: pedestrians, with walking speed 3 km/h, and cars with driving speed 40 km/h. Simulation results demonstrate that the proposed scheme made improvements in terms of the number of handovers by 30%.

In [33], a conditional random field (CRF)-based method was proposed by Zhang *et al.* for predicting the optimal serving base station. The proposed scheme is called CRF-cell selection protocol (CRF-CSP) and it relies on setting up a grid that covers the area of interest in the 3D space. The CRF-CSP is based on localization information to find the nearest grid point. In the model training phase, the optimal cell identifications and SINR values are given. Simulation results demonstrate that the proposed CRF-based method can predict the optimal base station with a high prediction accuracy (90%). In addition, it has superiority over other simple heuristic schemes.

A machine learning-based user association scheme is proposed by Zappone *et al.* [34]. It aims to maximize sum date rates achieved by users in massive multiple-input and multiple-output (MIMO) networks. The best serving base station is predicted using a trained model based on a feed-forward artificial neural network (FF-ANN). The geographical locations of users are given to the ANN model as inputs. The FF-ANN is structured as four fully connected layers with neurons of 128, 64, 64, and 40 respectively. The Rectified Linear Unit (ReLU) activation function is employed in the first and the third layers, while a sigmoidal activation function is used in the second layer of the FF-ANN. The adaptive moment (ADAM) estimation algorithm, which is a method for stochastic optimization, is used with Nesterov momentum for training the model [35]. The number of samples is 155,000, which is split into a training set of 140,000 samples and a validation set that includes 15,000 samples. Numerical results prove that the proposed method significantly reduces the computational complexity of the user association compared to the traditional cell selection scheme and it achieves the same performance as the traditional approach.

A user association approach was proposed by Elkourdi *et al.* [36] for two-tier HetNets. It solved the cell selection issue by applying a Bayesian game model between two players, i.e., user equipment (UEs) and access nodes (AN). The UE can be either delay-sensitive (DS) or delay-tolerant (DT), based on their delay requirement. Simulation results show that the proposed approach outperformed the conventional and cell-range-expansion (CRE) schemes in terms of the probability of proper cell selection and end-to-end latency.

Khan *et al.* introduced an ML-based cell selection approach for vehicles in mmWave networks in [37]. Distributed deep reinforcement learning (DDRL) is used to solve the vehicle association problem. The reinforcement learning problem is formulated as a Markov decision process (MDP). An Asynchronous Advantage Actor Critic (A3C) framework is used that includes actor and critic. Actions are sent from roadside units (RSUs) to a central entity that is responsible for calculating rewards to the RSUs. The proposed scheme decreases the control overhead and the computational complexity compared with other complex methods. Numerical results show that the proposed DDRL-based scheme has superiority over many cell selection schemes in terms of achievable sum rate by up to 15%.

Liu *et al.* proposed a cell selection approach that integrates the advantages of fuzzy logic and multiple attribute decision-making algorithms to perform the BS selection task in [38]. It depends on the Technique for Order Preference by Similarity to Ideal Solution (TOPSIS). The best serving BS is chosen based on several network parameters; reference signal receiving power (RSRP), SINR, and jitter. A subtractive clustering algorithm is applied to generate a suitable fuzzy membership function. The simulation results demonstrate that the overall performance of the proposed strategy is better than the RSS-based schemes. It enhances the network performance in terms of the number of handovers by almost 90% and the rate of ping-pong handovers by 10%, while providing an optimal Quality of Service (QoS) level.

In [39], Waheidi *et al.* proposed a distributed multi-class user association algorithm, known as Cell Association based on a Multi-Armed Bandit (CA-MAB) game. Static and mobile environments are considered in this work. User equipment and low- powered IoT devices are the classes that are

focused on. The evaluation results demonstrate that the proposed CA-MAB algorithm improves energy saving and the aggregated throughput. In addition, the mobility of devices affects equilibrium, throughput, and energy efficiency.

Zhang *et al.* introduced a deep learning-based cell selection scheme designed for ultra-dense networks in [40]. A two-tier heterogeneous ultra-dense Network was considered, consisting of macro- and small BSs. It aimed to solve the cell selection problem based on base station load. A U-Net convolutional neural network (CNN) was trained to select the optimal base station by mapping channel gain values onto images. Simulation results showed that the proposed CNN-based approach improved network robustness and decreased the computation time.

In [41], Sun *et al.* introduced two coordinated multi-point (CoMP) handover schemes for heterogeneous ultra-dense networks. The schemes are called movement-aware CoMP handover (MACH) and improved MACH (iMACH). They are based on estimating a dwell time of a user inside a serving cell. The MACH approach chooses n BSs that have the strongest received power with dwell time longer than a predefined threshold. The iMACH scheme selects $n-1$ BSs, as performed by the MACH scheme, and adds the nearest BS. In the MACH scheme, the handover is initiated when the farthest base station in the cooperating BSs set becomes the closest; in contrast, the handover is performed under the iMACH scheme when the closest BS becomes the farthest one. Simulation results shows that the proposed schemes improved the average throughput and the coverage probability and decreased the handover rate.

In [42], a user association method, known as HO RTP, was developed by Qin *et al.* for 5G ultra-dense networks. It selects base stations based on estimating the residence time inside a cell, where a predefined time threshold is set. The base station that has the strongest received signal power with a residence time longer than the predefined time threshold will be chosen as a serving BS. Simulation results prove that the proposed HO RTP scheme outperforms the conventional scheme in terms of average throughput achieved by users.

Alablani and Arafah proposed an adaptive cell selection (ADA-CS) approach for two-tier HetNets in [12]. It selects the optimal serving base station based on the various characteristics of network cells and vehicle movements. It performs six phases to achieve the cell selection task: configuration, decision-making, filtering, Handover based on Resident Time Prediction (HO narrowing, selecting, and handover triggering. Simulation results show that the proposed ADA-CS approach outperforms the traditional and recent cell selection schemes in terms of average achievable downlink data rates and spectral efficiency per vehicle by up to 3.98%. Moreover, it decreases the number of handovers by up to 42.39%.

The limitations of recent cell selection works that are presented in this section are:

- Most recent works follow a static, non-adaptive, strategy to select the serving base stations. As there are multiple tiers in HetNets, adaptive selection is preferred that can be performed by setting up certain thresholds to switch between the network tiers. For high-speed vehicles, macro- BSs are desired to maintain the network performance. On other hand, low- and medium-speed vehicles will be based on small BSs as the serving BSs.
- Most recent works give the highest priority to BSs that have the greatest receiving power to enhance the achievable throughput. In fact, in mobility environments, the closest BS that has the strongest receiving power will be far away when the user is moving forward. Therefore, relying on this principle leads to a degraded network performance due to unnecessary handovers.
- Some works depend on the estimation of the cell staying time, which is an essential factor of the serving cell selection. Moreover, these works, for simplicity purposes, estimate the staying time based on the assumption the user is at the edge of the cell.
- The number of ML-based works is fewer than the non-ML-based works, whereas predicting serving BSs needs to be based on machine learning algorithms to reduce the computational complexity. Moreover, input features for a machine learning model should be set carefully so that the trained model can solve the cell selection problem efficiently.
- Applying a cell selection strategy in a real-world context is preferable to study the effectiveness of the proposed protocol. Some works were tailored to certain typologies and applying them to a real-world case will lead to undesirable network performance.

Based on the limitations mentioned above, there is a need for cell selection methods that are adaptable for selecting the serving cell to be associated with in order to maintain network performance. In addition, relying on machine learning algorithms is a trend nowadays that we should take advantage of to reduce the computational complexity and prediction time. Furthermore, implementing a proposed cell selection algorithm on a realistic environment is desirable to determine the effectiveness and applicability of the proposed strategy.

III. THE PROPOSED A2T-KNN SCHEME

In this section, the proposed A2T-KNN scheme is discussed in terms of the SDN/ML-based model building process and the framework of the proposed approach.

A. THE PROPOSED SDN/ML-BASED MODEL BUILDING

To build the proposed machine learning model, five main stages have been passed through, as shown in figure 5 which are:

- **Stage 1: Data Preparation:** This stage aims to collect, generate and prepare information from vehicles and from macro- and small base stations. At the end of this stage, data that is essential to train and validate the proposed machine learning model will be ready.
  1) **BSs Dataset Collecting:** In this step, the appropriate dataset for the macro and small base stations

TABLE 1. Comparison among recent related cell selection studies.

Cite	Year	Authors	Designed for	ML-Based	Real-Word
[28]	2016	Arshad, R. et al.	Single and two-tier networks	No	No
[29]	2016	Tesema, F. B. et al.	Single-tier networks	No	No
[30]	2017	Cacciapuoti A. S.	Single-tier networks	No	Yes
[31]	2018	Wickramasuriya, D. et al.	Single-tier networks	Yes	No
[32]	2018	Kishida, A. et al.	Multi-tier networks	No	Yes
[33]	2018	Zhang, S. et al.	Single-tier networks	Yes	No
[34]	2018	Zappone, A. et al.	Single-tier networks	Yes	No
[36]	2019	Elkourdi, M. et al.	Two-tier networks	No	No
[37]	2019	Khan, H. et al.	Single-tier networks	Yes	No
[38]	2019	Liu, Q. et al.	Single-tier networks	No	No
[39]	2020	Waheidi, Y. M. et al.	Single-tier networks	No	No
[40]	2020	Zhang, Y. et al.	Two-tier networks	Yes	No
[41]	2021	Sun, W. et al.	Single-tier networks	No	No
[42]	2021	Qin, Z. et al.	Single-tier networks	No	No
[12]	2021	Alablani, I. A. and Arafah, M. A.	Two-tier networks	No	No

should be collected. BSs dataset can be found over the web as a single dataset that saves information related to both of macro and small BSs. On other hand, the macro and small BSs information may be found as two separated databases. The geographical location information of BSs in terms of latitude and longitude coordinates must be exist in the BS dataset. The collected BSs dataset that is used in this work is described in section IV-B.

2) **Vehicle Dataset Generation:** In this step a vehicle dataset is generated using Google Maps and MATLAB simulator. The explanation of vehicle dataset generation process is given in details in section IV-B.
3) **Data Cleaning and Labeling:** In the cleaning step, the data that is not used by the proposed cell selection scheme to predict the next BS is removed. It is worth mentioning that the central area of London has a high density of small cells, with a number of the traditional macro- cells, which makes the area suitable for our study. The labeling process is performed based on the A2T scheme that is described in Algorithm 1, where $\mathbb{BS}s_{small}$ and $\mathbb{BS}s_{macro}$ represent the small and macro- BSs. The vehicle speed threshold, the received signal strength indicator threshold, and the BS's load threshold are expressed by $\hat{S}$, $\hat{RSSI}$, and $\hat{L}$, respectively. The cell radius is denoted by R and the staying time of a vehicle within a cell is represented by ST_{ij}. The distance and azimuth between a base station B_i and vehicle V_j are represented by d_{ij} and Ω_{ij}.
4) **Data Dividing:** The data samples are divided into two datasets: a training set for ML model training and a testing set for model validation. In this work, an 80/ 20 (training/testing set) ratio was used. The training sample items were selected randomly from whole dataset and the testing sample was the remaining items.

Algorithm 1 Pseudocode for A2T Labeling Algorithm

input : $\mathbb{BS}s_{small}$, $\mathbb{BS}s_{macro}$.
output: $\mathbb{BS}$.
if $Veh.kspeed < \hat{S}$ **then**
  ====== Select from small BSs tier ======
  $X = \{B_i | B_i \in \mathbb{BS}s_{small}$ & $RSSI_{ij} > \hat{RSSI}$ *and* $load < \hat{L}\}$;
  $ST_{ij} = \frac{d_{ij}\ cos(\Omega_{ij}) + \sqrt{R^2 - d_{ij}^2\ sin^2(\Omega_{ij})}}{s_i}$; $\forall\ B_i \in X$
  $\mathbb{BS} = \{B_i | B_i \in X$ & *has* $max(ST_{ij})\}$;
end
if *Length* $(\mathbb{BS} == 0)$ **then**
  ====== Select from macro BSs tier ======
  $X = \{B_i | B_i \in \mathbb{BS}s_{macro}$ & $RSSI_{ij} > \hat{RSSI}\}$;
  $\mathbb{BS} = \{B_i | B_i \in X$ & *has* $max(RSSI_{ij})$;
end

- **Stage 2: ML Model Training:** In this stage, the machine learning model was trained using the training sample. In this work, the following ML models were trained to perform multi-classification based on supervised learning using a training set.
  - **K-Nearest-Neighbor (KNN):** This is a widely used and effective classifier, based on a predefined parameter (K) to determine the number of neighbors used in a similarity calculation that depends on the distance between samples. In this work, to measure the distance between two samples, the Euclidean distance is used.
  - **Feed-Forward Back-Propagation Artificial Neural Network (FFBP-ANN):** This is a popular machine learning algorithm that simulates the human neuron system. It is implemented based on feed-forwarding of data and back-propagation of errors. In this study, an FFBP-ANN is structured as three layers; input, hidden, and output. The number of neurons in the hidden layer is ten, while the number of neurons in the output layer is 658,

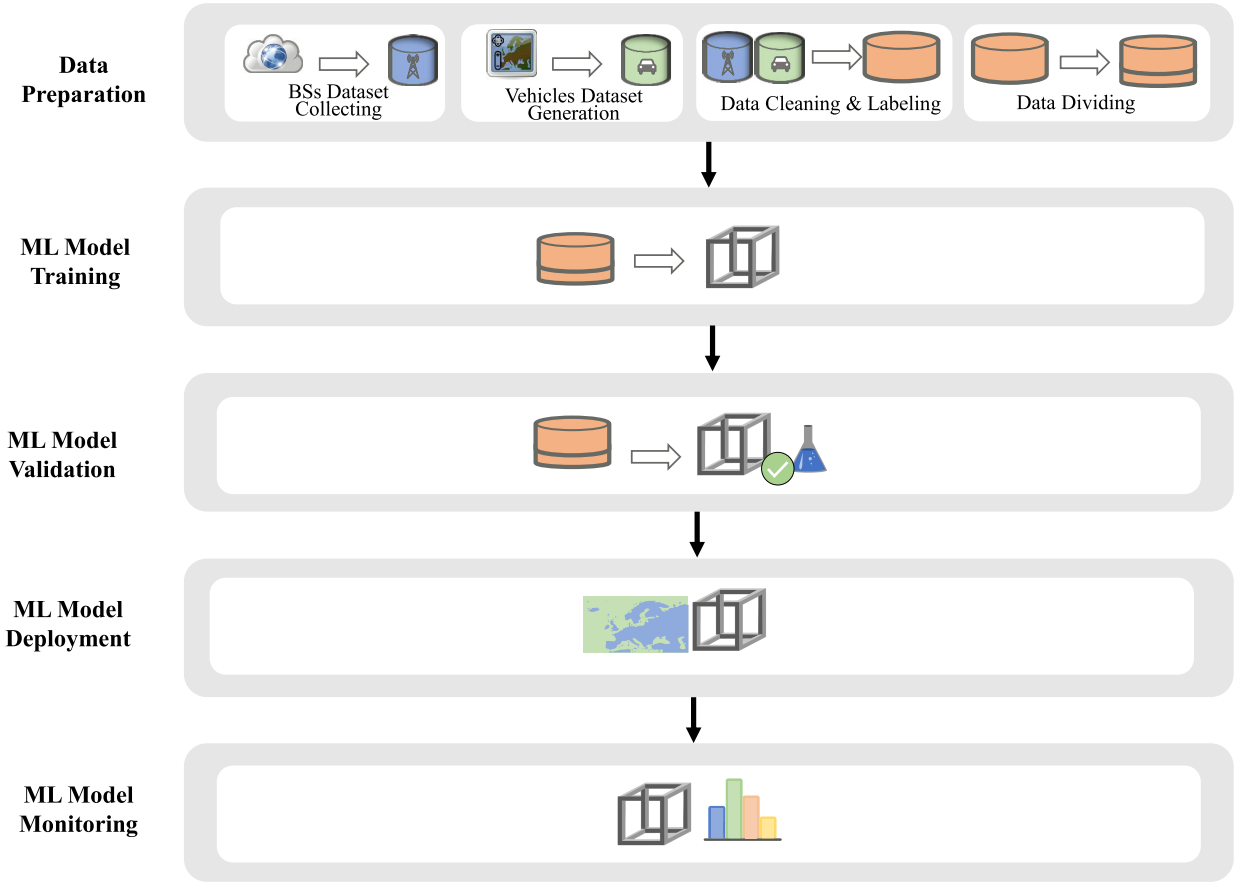

FIGURE 5. Stages for building the proposed ML model.

which equals the summation of the number of small and macro BSs. The activation function used is *tansig* and the training of the FFBP-ANN took approximately 17 days, using a high-performance computer.

– **Naive Bayes (NB):** This is a simple probabilistic classifier based on Bayesian law. In this work, the NB model is trained to predict the next BS.

- **Stage 3: ML Model Validation:**The proposed ML classifiers were tested using the testing sample. The performance of the trained ML models is described in detail in section V-A. The KNN classifier outperforms the FFBP-ANN and NB classifiers in terms of prediction efficiency. Therefore, the KNN trained model is selected in this work to be the BS prediction tool.
- **Stage 4: ML Model Deployment:** ML model deployment is the process of installing the trained ML model on the SDN controller. The SDN controller is the core component of an SDN-based vehicular network, and is physically connected to network elements, including wireless base stations [43], [44]. It is responsible for performing the adaptive cell selection task based on the installed ML model.
- **Stage 5: ML Model Monitoring:** In this stage, the proposed ML model was evaluated to monitor its performance in a real-world case based on London. Section V-B represents the evaluation of the proposed A2T-KNN in terms of average number of handovers, staying time, number of HO failures and unnecessary HOs, downlink sum-rate, energy efficiency, radio link failures, and HO interruption time.

B. FRAMEWORK OF THE PROPOSED SDN/ML-BASED CELL SELECTION APPROACH

The framework is based on the combined SDN and ML approach, as shown in figure 6. SDN is applied to perform efficient traffic management and cell selection tasks, based on the installed trained machine learning model. The inputs of the ML-model are vehicle information and network configuration information. The geographical coordinates of vehicles (i.e., latitude (*LAT*) and longitude (*LON*)), azimuth between vehicle direction and the north (*AZIMUTH*), and

Algorithm 2 Pseudocode for A2T-KNN Algorithm

input : $Veh.lat$, $Veh.lon$, $Veh.azimuth$, $Veh.kspeed$, $\hat{L}$, $\hat{S}$, $R\hat{S}SI$, R.
output: $\mathbb{BS}$.
while *Vehicle moves* **do**
  if $RSSI < Th$ || $len(\mathbb{BS}) == 0$ **then**
    $Input = [Veh.lat, Veh.lon, Veh.azimuth, Veh.kspeed, \hat{L}, \hat{S}, R\hat{S}SI, R]$;
    $\mathbb{BS} =$ KNNMdl $(Input)$;
    Trigger handover to BS# $\mathbb{BS}$;
  end
end

TABLE 2. Description of the dataset of the UK BSs.

Number of columns	12
Names of columns	'Operator','Opref','Sitengr', 'Antennaht','Transtype', 'Freqband','Anttype', 'Powerdbw','Maxpwrdbw', 'Maxpwrdbm','Sitelat', 'Sitelng'
Number of rows	144,557

vehicle speed in km/h (*KSPEED*) are given to the ML model. In addition, the predefined BS's load, vehicle's speed, RSSI, and cell radius thresholds are also inserted into the ML model. Based on the given information, the ML model can predict the optimal BS to be associated with, whether it is a macro- or small BS. Algorithm 2 gives the pseudocode for the proposed A2T-KNN scheme.

IV. SYSTEM MODEL

A. SIMULATION TOOL

The MATLAB 2021a simulator was used for modeling and analyzing the performance of the proposed cell selection scheme due to its powerful capabilities. In addition, THE MATLAB simulator has many toolboxes that can be used to perform the cell selection task in a realistic environment. Figure 7 shows the main MATLAB toolboxes that are installed to perform simulation experiments.

B. DATASETS

- **BSs dataset:** In [45], Boswarva created a dataset of point locations of wireless base stations located in the United Kingdom in February 2017. The raw data was publicly released by The Office of Communications (Ofcom), which is the UK's governmental communications regulator [46]. It has been uploaded on the Sitefinder website as a Microsoft Excel spreadsheet. A description of the UK BSs dataset is given in Table 2. In the dataset, there are six mobile network operators: Airwave, Orange, O2, T-Mobile, Three and Vodafone, as illustrated in figure 8.
- **Vehicles dataset:** A vehicle dataset of the central area of London was created by us in August 2021. This dataset was generated using Google Maps and the MATLAB simulator. The following processes were performed using Google Maps:
  - Starting Google My Maps, as shown in figure 9a.
  - Creating a new map of London (figure 9b).
  - Adding driving routes for the selected London streets (figures 9c and 9d): 55 streets were chosen in this work, as shown in Table 3. Each driving route has a set of geographical points.
  - Exporting the created driving routes as Keyhole Markup Language (KMZ) files (figure 9e).

  Using the MATLAB simulator, the following operations were performed:
  - Generating extra geographical points for each street, based on a predefined distance, which is 1 meter in this work.
  - Calculating the azimuth for each point according to the street on which the point is located. The azimuth is the angle between north and the street direction, beginning from the located point.
  - Generating random speeds in kilometers per hour (km/h) ranging from 10 to 40 km/h.
  - Exporting the vehicle dataset of the central area of London as a Microsoft Excel spreadsheet that has 38,441 rows.

  The description of the vehicle dataset fields is given in Table 3. Figure 10 shows a snapshot of the generated vehicle dataset.

C. NETWORK MODEL

A two-tier heterogeneous ultra-dense network is considered that is comprised of macro- and small BSs. The system model represents the distribution of base stations operated by Vodafone in the middle of London, as shown in figure 11. The set of base stations is denoted by $\mathbb{BS}s = \{B_1, B_2, \ldots, B_I\}$ and includes the macro- and small base stations, ($\mathbb{BS}s_{macro}$ and $\mathbb{BS}s_{small}$), respectively. Total network vehicles is expressed by $\mathbb{V} = \{V_1, V_2, \ldots, V_J\}$ and these vehicles are distributed within the central area of London. A vehicle can be connected to only a single BS at a time. The association matrix between base stations and vehicles is denoted by $\mathbb{A} = \{A_{11}, A_{12}, \ldots, A_{IJ}\}$, where the association variable between base station B_i and vehicle V_j is expressed by A_{ij} and it can take either 0 or 1.

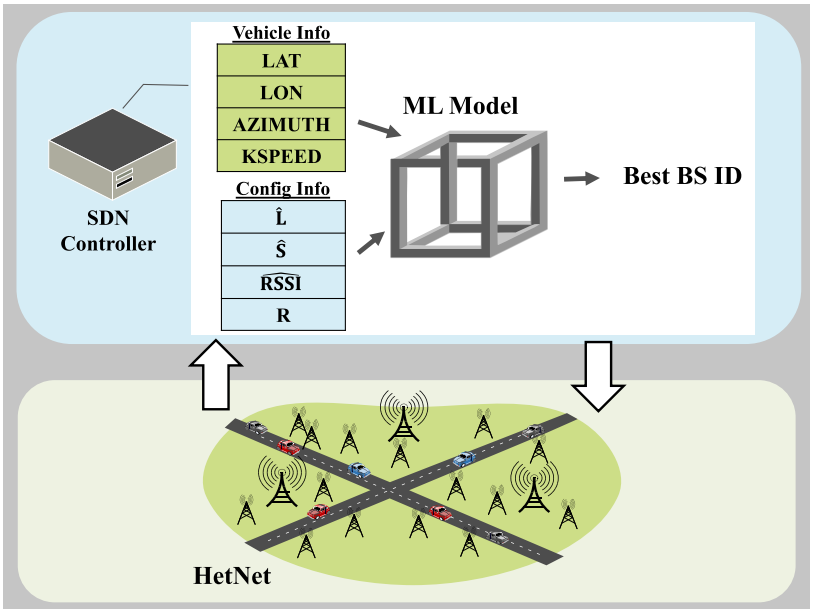

FIGURE 6. Framework of the proposed SDN/ML-based cell selection approach.

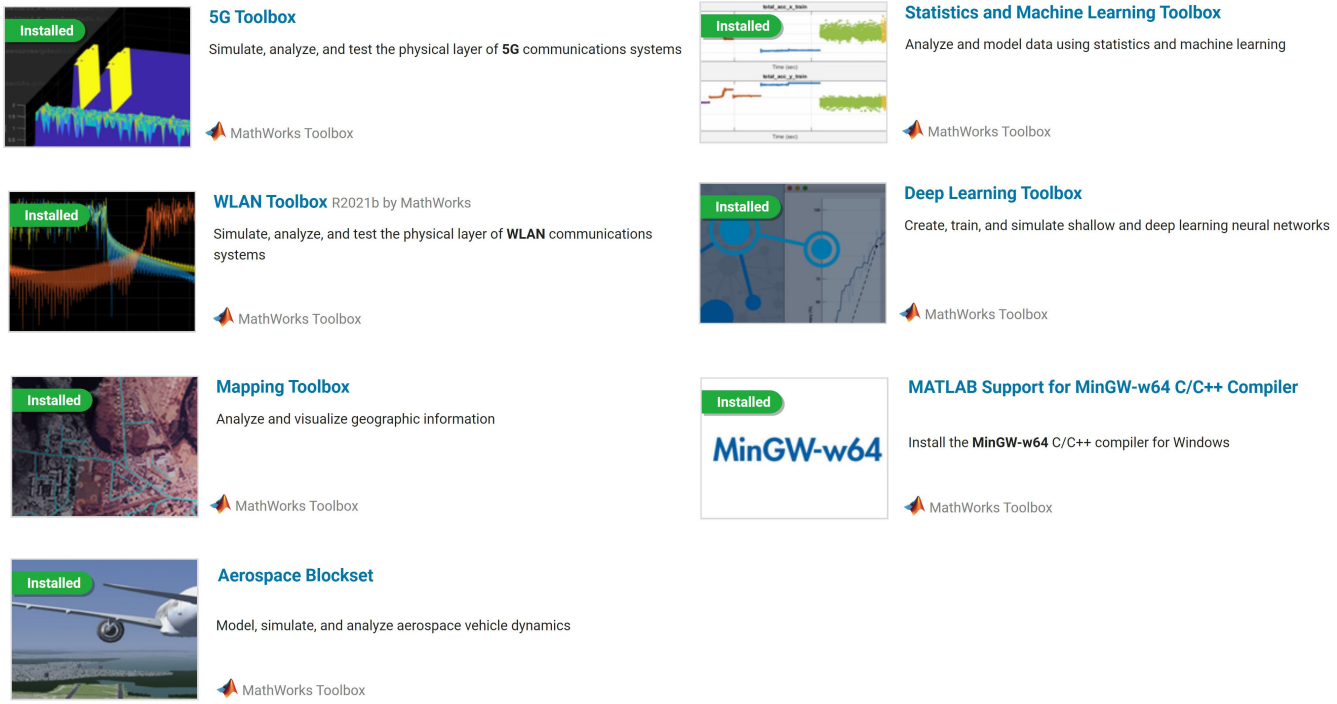

FIGURE 7. The MATLAB toolboxes used.

D. PROPAGATION MODEL

In this paper, the propagation channel model comprises three main components: path-loss (PL), fading and shadowing. These are the main losses that affect the strength and quality of wireless signals. The 3rd Generation Partnership Project (3GPP) path loss models are used to estimate the received signal strength at a given distance from the serving base station. Table 4 shows the used 3GPP path loss models that

TABLE 3. Description of the generated London vehicle dataset.

Field Name	Description	Values
'STREET_NAME'	Name of London street where vehicle is located.	'Aldgate','Bethnal Green','Bevis Marks','Brick Ln', 'Brook','Cable','Cannon','Chancery Ln','City','Clerkenwell','Commercial', 'Coventry','Crawford','Epworth','Euston','Farringdon','Finsbury Square','Fleet','George','Gower','Grays Inn','Great Marlborough','Grosvenor Square','Grosvenor','Hackney','High Holborn','Holborn','Hollest','Lever','Lime','Lisson Grove','London Wall','Long Acre','Marylebone','New Cavendish','New Oxford','New','Northington','Old Gloucester','Orange','Oxford','Park','Portland Pl','Queen Square',"Regent',Riding House','Rosebery Ave','Seymour','Shaftesbury Ave','Strand','Tottenham Court','Voss','Whitechapel','Wilson','York'
'LAT'	Latitude coordinate of vehicle.	[51.51 to 51.53]
'LON'	Longitude coordinate of vehicle.	[-0.1693 to -0.0538]
'AZIMUTH'	Angle between vehicle direction and north in degrees.	[0 to 357.2597]
'KSPEED'	Speed of vehicle in km/h.	[10 to 40]

FIGURE 8. The mobile network operators in the UK BSs dataset.

are defined in 3GPP technical report (TR) 38.901 version 16.1.0 [47]. As shown in the table, the macro- BSs tier uses the urban macro-cell-non-line-of-sight (UMa-NLOS) PL model, while the small BSs tier uses urban microcell-line-of-sight (UMi-LOS) (street canyon) model.

The carrier frequency is denoted by f_c and it is measured in Gigahertz. The distance between a base station and a vehicle is represented d and it is measured in meters. The definition of break-point distance (d'_{BP}) is given in equation (1).

$$d'_{BP} = 4\,(h_{BS} - h_{Eff})\,(h_{Veh} - h_{Eff})\,f_c/c \tag{1}$$

The heights of a BS and a vehicle are expressed as h_{BS} and h_{Veh}, respectively. The vehicles' height must be between 1.5 and 22.5 meters to apply the 3GPP PL models. The effective height between vehicles and BSs is indicated by h_{Eff} and it is described in detail in the technical report. The symbol c represents the speed of light in a vacuum, which equals 2.997 x 10^8 ms^{-1}.

Rayleigh fading is considered in our study because it is a good approximation of realistic conditions of a wireless channel. It follows an independent exponential distribution with unit mean [48]. In addition, log-normal shadowing is considered because it is typically used to model the relationship between RSSI and range [49].

V. PERFORMANCE ANALYSIS

In this section, the trained ML models are evaluated to determine how well they classify input data that the models were not trained on. Moreover, the proposed A2T-KNN algorithm is evaluated in terms of the average number of handovers, staying time, number of HO failures and unnecessary HOs, downlink sum-rate, and energy efficiency.

A. EVALUATION OF THE TRAINED ML MODELS

Table 5 shows the number of training and testing samples that are used in this work. Root mean square error (RMSE) and mean absolute error (MAE) are common criteria for measuring errors in prediction [27], [50]. The calculation of RMSE and MAE is based on the predicted base stations ($\hat{y}$), the target BSs (y), and the number of testing samples (N), i.e., 7,689 samples. A confusion matrix is an effective tool to summarize classification results in a tabular form, where the results of classes are tallied [51]. Based on the constructed confusion matrix, the numbers of true positive (TP), false positive (FP), true negative (TN) and false negative (FN) observations were calculated [52]. Then, accuracy, sensitivity, specificity, precision, F-measure (F1), and geometric mean (G-mean) were estimated. Table 6 illustrates the evaluation values of the trained ML models, i.e., KNN, FFBP-ANN, and NB models. The results demonstrate that the KNN model achieves a high prediction performance with low percentages of error. Thus, it is chosen to be the used ML model.

B. EVALUATION OF THE PROPOSED A2T-KNN SCHEME

1) KEY PERFORMANCE INDICATORS

The key performance indicators (KPIs) that were used to evaluate the performance of the proposed A2T-KNN algorithm were the average number of handovers, staying time, number of HO failures and unnecessary HOs, downlink sum-rate, energy efficiency, radio link failures, and handover interruption time.

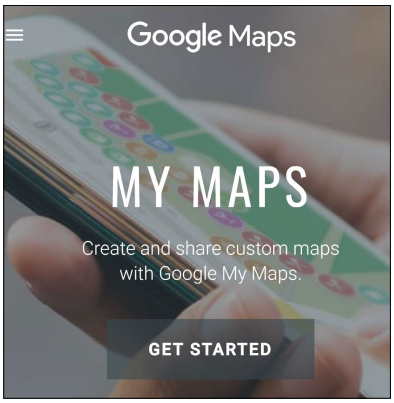

(a) Starting Google My Maps

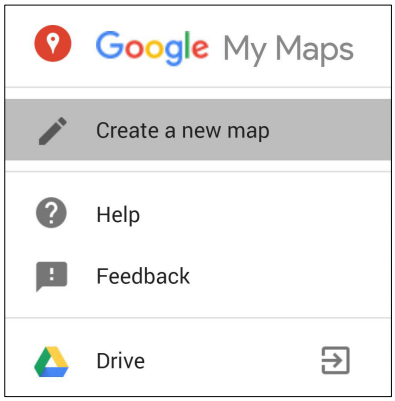

(b) Creating a new map.

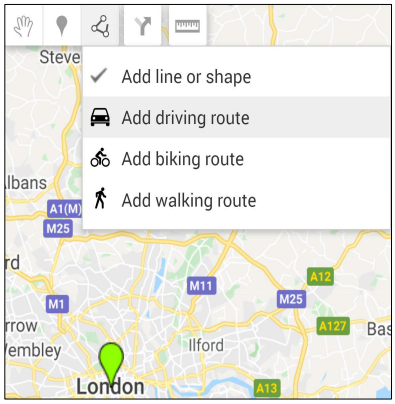

(c) Adding driving route.

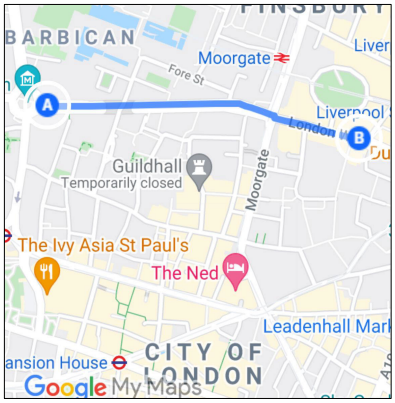

(d) Drawing the start and end points of a route.

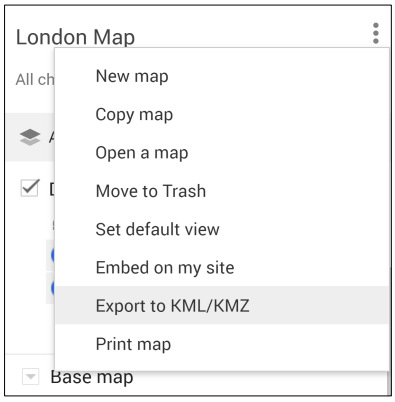

(e) Exporting the route as a KMZ file.

FIGURE 9. Using Google Maps to create a driving route.

Handover is the process of switching the connection between network cells when a mobile device moves out of the range of the current serving cell [53]. There are two kinds of handovers: horizontal and vertical HOs. A horizontal HO occurs between homogenous base stations, while a vertical HO happens between heterogeneous BSs [54], [55]. Decreasing the number of handovers incurred by a vehicle is an important factor to maintain the network performance [56]. The number of HOs depends on the staying period of a vehicle within a serving cell, as the longer the stay time, the lower the number of HOs [57]. When the handover delay is longer than the staying time within a cell, a handover failure happens. When the sum of HO delays to move into (t_i) and out (t_o) of the network cell is longer than the staying time in a cell, an unnecessary handover occurs [12], [58]. Equations (2) and (3) show the formulas for the probability of a HO failure

TABLE 4. The used 3GPP path loss models.

Macro BSs tier	PL model	3GPP UMa-NLOS
	Equations	$\zeta(d) = max(\zeta(d), \zeta^{'}(d))$ where $\zeta(d) = \begin{cases} 28 + 22\ log_{10}(d) + 20\ log_{10}(f_c) & 10\ m \leqslant d \leqslant d^{'}_{BP} \\ 28 + 40\ log_{10}(d) + 20\ log_{10}(f_c) - 9\ log_{10}((d^{'}_{BP})^2 + (h_{BS} - h_{Veh})^2) & d^{'}_{BP} \leqslant d \leqslant 5\ km \end{cases}$ $\zeta^{'}(d) = 13.54 + 39.08\ log_{10}(d) + 20\ log_{10}(f_c) - 0.6\ (h_{Veh} - 1.5)$
Small BSs tier	PL model	3GPP UMi-LOS (street canyon)
	Equations	$\zeta(d) = \begin{cases} 32.4 + 21\ log_{10}(d) + 20\ log_{10}(f_c) & 10\ m \leqslant d \leqslant d^{'}_{BP} \\ 32.4 + 40\ log_{10}(d) + 20\ log_{10}(f_c) - 9.5\ log_{10}((d^{'}_{BP})^2 + (h_{BS} - h_{Veh})^2) & d^{'}_{BP} \leqslant d \leqslant 5\ km \end{cases}$

Veh_Table.xlsx

	A	B	C	D	E
	VehTable				
	street_name	lat	lon	azimuth	kspeed
	Categorical	Number	Number	Number	Number
1	street_name	lat	lon	azimuth	kspeed
2	Aldgate St	51.5145	-0.0741	59.7011	10
3	Aldgate St	51.5144	-0.0743	59.4935	15
4	Aldgate St	51.5143	-0.0746	60.1489	25
5	Aldgate St	51.5142	-0.0747	60.6460	40
6	Aldgate St	51.5141	-0.0751	61.8252	40
7	Aldgate St	51.5141	-0.0752	56.1963	15
8	Aldgate St	51.5140	-0.0753	63.3363	40
9	Aldgate St	51.5139	-0.0758	61.8253	40
10	Aldgate St	51.5138	-0.0761	66.6057	25
11	Aldgate St	51.5137	-0.0763	90.0000	35
12	Aldgate St	51.5137	-0.0763	51.2204	10
13	Aldgate St	51.5137	-0.0764	68.1138	20
14	Aldgate St	51.5136	-0.0766	61.8255	40
15	Aldgate St	51.5136	-0.0766	61.8255	35
16	Aldgate St	51.5136	-0.0766	51.2204	40
17	Aldgate St	51.5136	-0.0766	69.6544	30

FIGURE 10. Snapshot of the generated vehicle dataset.

TABLE 5. Number of training and testing samples.

Number of training samples	30,752
Number of testing samples	7,689

and unnecessary HO, respectively.

$$Pr_f = \begin{cases} \frac{2}{\pi}[\sin^{-1}(\frac{vt_i}{2R}) - \sin^{-1}(\frac{vTh_f}{2R})], & 0 \leqslant Th_f \leqslant t_i \\ 0, & t_i < Th_f \end{cases} \quad (2)$$

$$Pr_u = \begin{cases} \frac{2}{\pi}[\sin^{-1}(\frac{v(t_i + t_o)}{2R}) - \sin^{-1}(\frac{vTh_u}{2R})], \\ \qquad 0 \leqslant Th_u \leqslant (t_i + t_o) \\ 0, \qquad (t_i + t_o) < Th_u \end{cases} \quad (3)$$

where vehicle velocity and cell radius are denoted by v and R. The time thresholds of a HO failure and unnecessary HO are represented by Th_f and Th_u. They can be calculated according to equations (4) and (5), where the acceptable values of Pr_f and Pr_u are 0.02 and 0.04.

$$Th_f = \frac{2R}{v} sin(\sin^{-1}(\frac{vt_i}{2R}) - \frac{2}{\pi} Pr_f); \quad 0 \leqslant Pr_f \leqslant 1 \quad (4)$$

$$Th_u = \frac{2R}{v} \sin(\sin^{-1}(\frac{v(t_i + t_o)}{2R}) - \frac{2}{\pi} Pr_u); \quad 0 \leqslant Pr_u \leqslant 1 \quad (5)$$

The average number of HO failures ($\overline{N_f}$) and unnecessary HO ($\overline{N_u}$) can be estimated as shown in equations (6) and (7).

$$\overline{N_f} = Pr_f \times \overline{N_{HO}} \quad (6)$$

$$\overline{N_u} = Pr_u \times \overline{N_{HO}} \quad (7)$$

Small cell densification is a promising solution that can be used to fulfil the 5G network requirements of network capacity and throughput [59]. The total aggregate throughput (sum rate) is the summation of the achievable data rate across the network when a vehicle moves [41], as equation (8) shows. Channel capacity C_{ij} between base station B_i and vehicle V_j can be calculated based on the Shannon theorem as given in equation (9).

$$Sum\ R_j = \sum_i C_{ij} \quad \forall\ B_i \in \mathbb{BS}s. \quad (8)$$

$$C_{ij} = BW\ \ log_2(1 + \psi_{ij}) \quad (9)$$

The signal-to-interference-plus-noise ratio is defined as the power received from the serving BS divided by the summation of the power received from other BSs plus noise [60]. It is represented by ψ_{ij} and its formula is given in equation (10).

$$\psi_{ij} = \frac{p_{tx_i} \zeta_{ij}(d) g_{ij}}{\sum_{m \neq i}(p_{tx_m} \zeta_{mj}(d) g_{mj}) + N_0 BW}, \quad \forall\ B_i \in \mathbb{BS}s\ and\ \forall\ V_j \in \mathbb{V}. \quad (10)$$

where p_{tx} is the maximum transmitting power of a base station, $\zeta(d)$ is the path loss function, and g represents the channel gain between BS and vehicle. As previously discussed in section IV-D, the path loss function follows the 3GPP PL models and the channel gain considers the impacts of

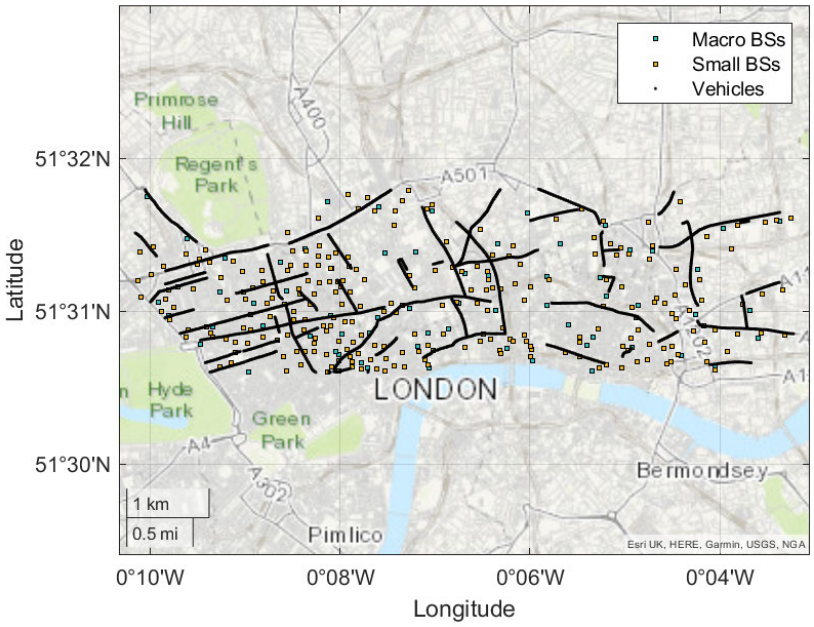

FIGURE 11. System model in central London.

TABLE 6. The trained ML models evaluation values.

Performance Metrics	Equation	KNN Model	FFBP-ANN Model	NB Model
RMSE	$\sqrt{\frac{\Sigma_{i=1}^{N}(\hat{y}_i - y_i)^2}{N}}$	57.54	126.31	129.70
MAE	$\frac{\Sigma_{i=1}^{N}\lvert y_i - \hat{y}_i\rvert}{N}$	50.86	50.85	57.66
Accuracy (%)	$\frac{TP+TN}{TP+TN+FP+FN}$	99.91	99.77	99.73
Sensitivity (%)	$\frac{TP}{TP+FN}$	88.05	69.71	63.31
Specificity (%)	$\frac{TN}{FP+TN}$	99.95	99.88	99.86
Precision (%)	$\frac{TP}{TP+FP}$	88.05	69.71	63.31
F1 (%)	$\frac{TP}{TP+0.5\ (FP+FN)}$	88.05	69.71	63.31
G-mean (%)	$\sqrt{(Sensitivity \times Specificity)}$	93.81	83.44	79.51

Rayleigh fading and log-normal shadowing. The noise power spectral density and sub-channel bandwidth are denoted by N_0 and BW, respectively. They are used to estimate the thermal noise level, based on an additive white Gaussian noise model.

The energy efficiency (EE) of the system is a critical evaluation criterion and it refers to the ratio between the sum of the achievable data rate and the total consumed power [61]. Equation (11) gives the formula for the energy efficiency, which is denoted by η_{EE}.

$$\eta_{EE}\ (bits/joule) = \frac{Sum\ of\ achievable\ rate\ (bps)}{Total\ consumed\ power\ (Watt)} \quad (11)$$

The quality of the radio link is modeled in the term signal-to-interference-plus-noise ratio. Radio link failure occurs when the value of SINR of a vehicle V_j from the serving cell B_j falls below the out-of-synchronization threshold (SYN_{out}) for a Radio Link Failure (RLF) detection period, which is known as T_{RLF}. If T_{RLF} timer, which is also known as T310, has expired and the SINR value does not increase above the in-synchronization threshold (SYN_{in}), the vehicle faces a problem of RLF. Equations (12) and (13) shows the conditions of failure and recovery of radio link [62], [63].

$$C_{RLF} : \psi_{ij} < SYN_{out};\ \ for\ t_{out} > T_{RLF} \quad (12)$$

$$C_{Recovery} : \psi_{ij} > SYN_{in};\ \ for\ t_{in} > T_{RLF} \quad (13)$$

Handover interruption time (HIT) is an essential metric to evaluate the performance of cell selection schemes. HIT is defined as the duration in which the vehicle's connectivity is interrupted to perform the handover operation [64]. Equation (14) gives the formula of T_{HIT} which is the summation of break time (T_{Break}), processing time (T_{Proc}), interruption time ($T_{Interrupt}$), radio access channel time (T_{RACH}) and handover completion time (T_{HC}) [65].

$$T_{HIT} = T_{Break} + T_{Proc} + T_{Interrupt} + T_{RACH} + T_{HC} \quad (14)$$

2) SIMULATION RESULTS

In this section, the simulation results are presented and discussed. The performance of the proposed A2T-KNN is compared with the traditional max-RSSI, HO RTP [42], and Zappone *et al.* ANN- based [34] schemes. Table 7 displays the simulation parameters used to evaluate the cell selection schemes.

TABLE 7. Simulation parameters.

Simulation Parameters	Values	
	Macro BS	Small BS
Number of BSs	389	269
Carrier frequency (GHz)	2	28
System bandwidth (MHz)	10	500 [66]
Transmit power (dBm)	46	30
Path loss model (dB)	3GPP UMa Model	3GPP UMi Model
Standard deviation of shadow factor (dB)	6	4
Base station height (meters)	25	10
Cell radius (meters)	1400	600
SYN_{out} (dB)	-8	-12
T_{RLF} (sec)	1	
Vehicle speeds (km/h)	[10-40]	
Vehicle height (meters)	1.8	
RSSI threshold (dBm)	-80	
Speed threshold (km/h)	25	
Load threshold (%)	90	
Thermal noise density (dBm/Hz)	-174	
Shadowing	Log-normal	
Fast fading	Rayleigh fading	
Handover delay (sec)	1 [42]	
Simulation time (sec)	600	

Figure 12 displays the average staying time of vehicles under different driving speeds, while figure 13 shows the relationship between the average number of handovers and vehicle speeds. The results show that the staying time decreases as the speed of a vehicle increases, and therefore the number of HOs will increase. The proposed A2T-KNN algorithm is superior to the conventional scheme, which is based on the maximum RSSI values, and the HO RTP and Zappone *et al.* ANN-based methods in terms of average staying time and average number of HOs. The reason is that the proposed A2T-KNN selects the small BS that has the longest staying time when the vehicle speed is lower than a predefined speed threshold (25 km/h in this scenario). Exceeding the speed threshold leads to selecting the nearest macro BS to avoid

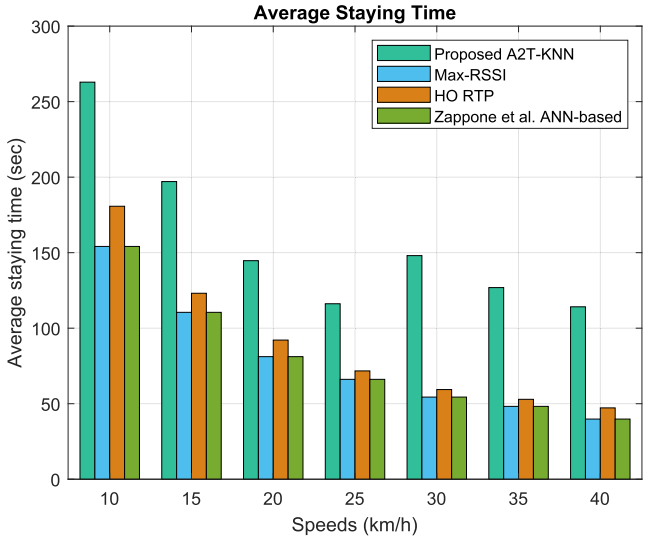

FIGURE 12. Average staying time vs vehicle speed.

unnecessary HOs. As the figures illustrate, the conventional max-RSSI and Zappone *et al.* ANN-based schemes are the least efficient in terms of staying time and involve the largest number of handovers. The max-RSSI method selects a base station that has the maximum RSSI values without considering the direction and speed of a vehicle. The Zappone *et al.* method uses a trained FF-ANN model to predict the next base station based on the principle of increasing the achievable sum-rate by relying on the shortest distance between a base station and a vehicle, regardless of the direction and speed of the vehicle. Consequently, our A2T-KNN outperforms the conventional and Zappone *et al.* methods in terms of average staying time and number of HOs by 42.68% and 45.83%, respectively, when the speed threshold is not exceeded. The HO RTP scheme selects the nearest small BS that has a residence time greater than a specific time threshold; as a result, the proposed A2T-KNN outperforms the HO RTP scheme in terms of the average staying time and number of HOs by 35.12% and 38.1%, respectively. This is because the HO RTP considers the residence period within the small cell, but it gives the highest priority in selection to the RSSI value. Moreover, the proposed AT2-KNN achieves additional enhancements regarding the average staying time and number of handovers with vehicles that exceed the speed threshold, due to the adaptation characteristic of the proposed algorithm.

The average number of HO failures and unnecessary HOs at different speeds are represented in figures 14 and 15. Increasing speed clearly leads to an increase in the average number of unsuccessful and unnecessary HOs. However, we found that the proposed A2T-KNN algorithm achieves the lowest mean numbers of HO failures and unnecessary HOs compared with the conventional max-RSSI, Zappone *et al.* ANN-based, and the HO RTP methods. The reason behind this is that the A2T-KNN scheme relies on

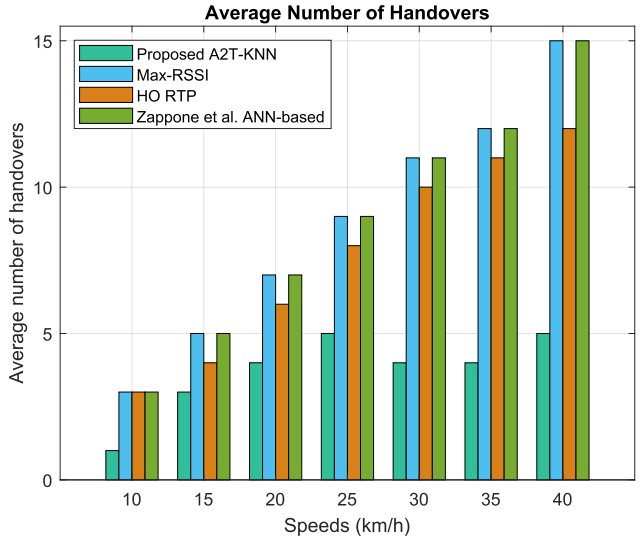

FIGURE 13. Average number of handovers vs vehicle speed.

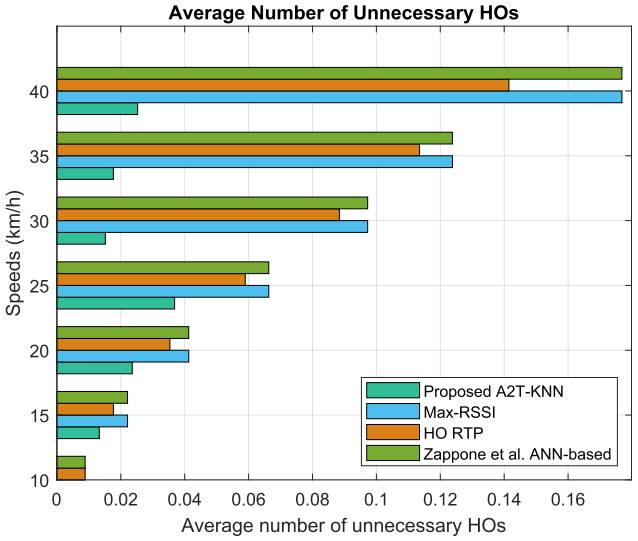

FIGURE 15. Average unnecessary HOs vs vehicle speed.

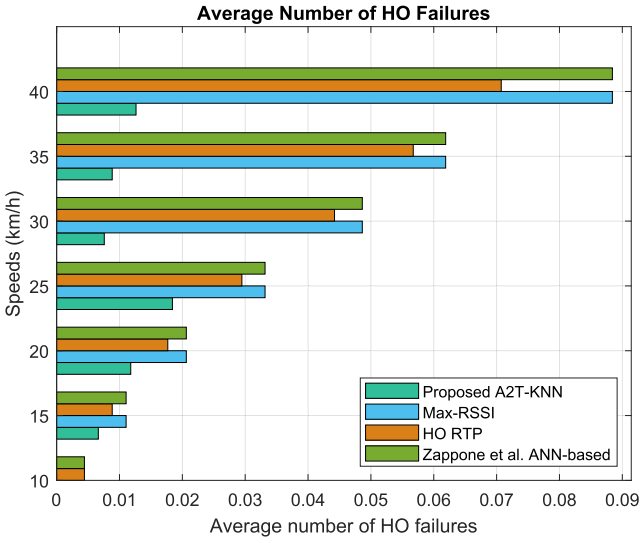

FIGURE 14. Average HO failures vs vehicle speed.

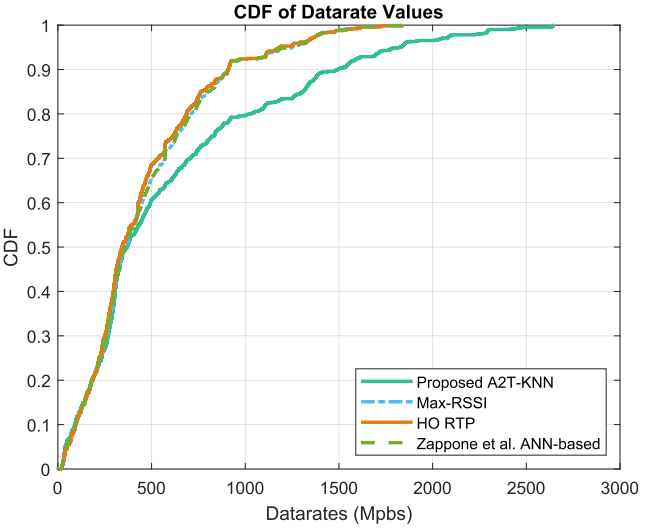

FIGURE 16. CDF of achievable downlink data rates by a vehicle during simulation time.

estimating the staying time accurately and it has the adaptation ability that allows switching between different BSs tiers in HetNets based on a specific speed threshold. Thus, the A2T-KNN outperforms the conventional max-RSSI and Zappone *et al.* ANN-based methods by 44.68% and the HO RTP method by 36.59% when the vehicle speed is lower than the speed threshold. Additional improvements were made by the A2T-KNN scheme when the vehicle speed exceeded the threshold due to the association switching to the macro-BS tier.

The cumulative distribution function (CDF) of achievable downlink data rate of a vehicle during the simulation time under a specific speed (10 km/h in this example) is represented in Figure 16. As the figure shows, the proposed A2T-KNN protocol reaches peaks in the data rates, while the max-RSSI, Zappone *et al.* ANN-based, and HO RTP schemes do not achieve these peaks. Using the A2T-KNN protocol, the movement of a vehicle forward leads to it approaching the mid-point of a serving wireless cell in which the BS is located, and thus the A2T-KNN can achieve the maximum possible value of the data rate. On the other hand, relying on signal strength values and giving them a high priority does not guarantee reaching the highest data rate values when vehicles move. Therefore, the A2T-KNN scheme is superior to the max-RSSI and Zappone *et al.* ANN-based methods in terms of the average achievable sum rate by 14.41% and has superiority over the HO RTP approaches by 17.18%.

Figure 17 illustrates the CDF of network energy efficiency for a vehicle during the simulation time. As the energy efficiency is the achievable sum data rate divided by total consumed power, the A2T-KNN algorithm is superior to the other cell selection strategies because it outperforms them

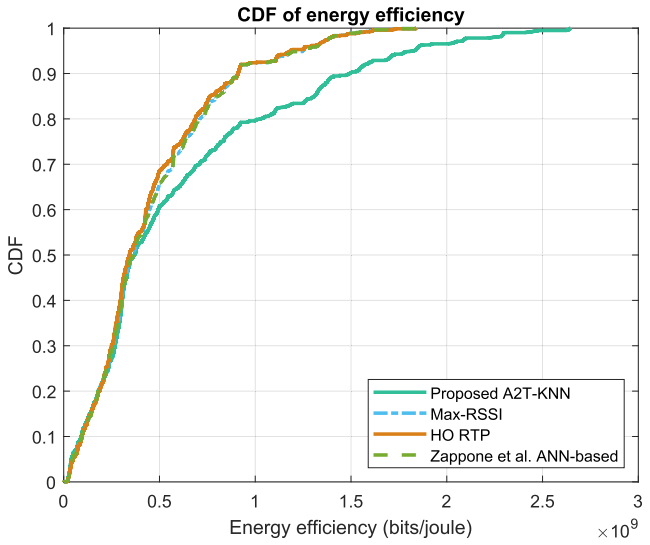

FIGURE 17. CDF of network energy efficiency achieved by a vehicle during simulation time.

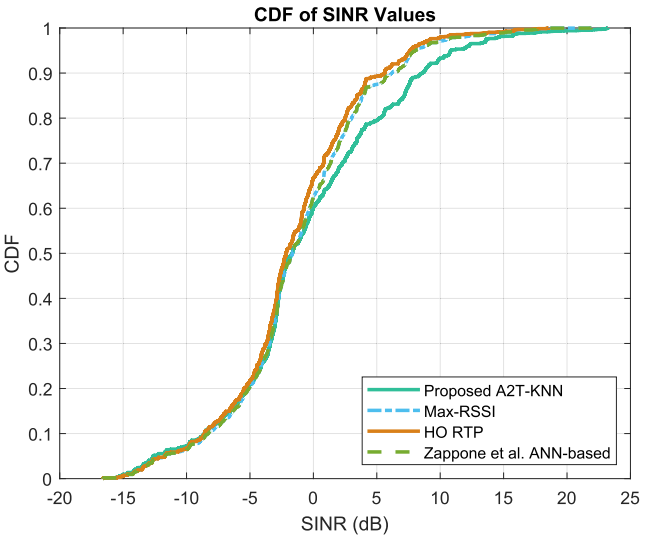

FIGURE 18. CDF of received SINR values by a vehicle during simulation time.

in terms of the total achieved downlink data rate, as illustrated in figure 16. The percentage of improvement in terms of average network energy efficiency achieved by vehicles is 13.99% compared with the conventional max-RSSI and Zappone *et al.* ANN-based methods, while A2T-KNN outperforms the HO RTP method by 16.86%.

Figure 18 shows the CDF of received SINR values by a vehicle during simulation time. According to the result, downlink SINR improves by applying our A2T-KNN scheme because it achieves high SINR values that are not reached using the other cell selection methods. We found that RLFs occur when SINR values drop below SYN_{out} for T_{RLF}, which does not exceed 1.67% using our A2T-KNN scheme and the other cell selection scheme. The reason for this is that all simulation experiments depend on setting an RSSI threshold and if the received RSSI value is less than this threshold, the cell selection algorithm is executed. In fact, radio link failures can be avoided by enhancing the SINR values by applying interference mitigation techniques. In addition, relying on soft handover, which means connecting to the next BS before breaking the old one, helps in reducing the RLF rate.

Figure 19 shows the relation between vehicle speed and average cumulative handover interruption time. As the figure shows, our proposed A2T-KNN scheme outperforms other methods because it aims to prolong the staying time of vehicles within serving cells and therefore decreases the cumulative HIT. In addition, the proposed scheme applies switching between the small BS tier and macro BS tier if the vehicle speed exceeds the predefined speed threshold to avoid frequent HOs. We find that the worst cell selection methods in terms of cumulative HIT are the Max-RSSI and Zappone *et al.* ANN-based schemes. The reason is that they depend on the strongest received RSSI value when they select the next BS, and therefore the number of HOs increases and the cumulative HIT gets worse. Our protocol outperforms

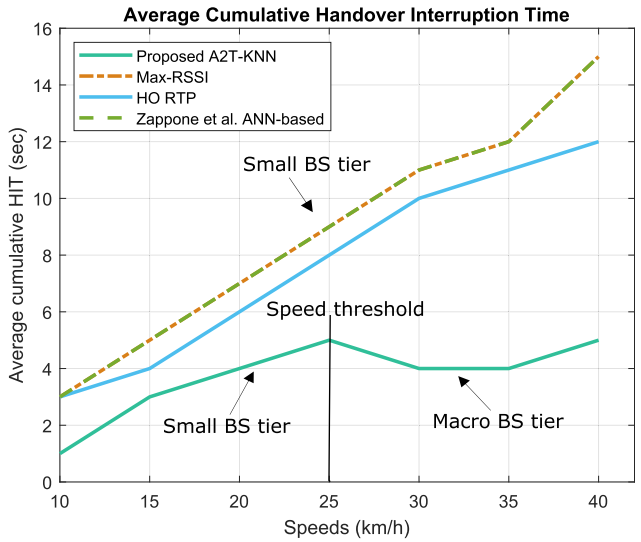

FIGURE 19. Average cumulative HIT vs vehicle speed.

them in terms of cumulative HIT by 45.83%. The HO RTP method achieves better performance in terms of cumulative HIT compared with the max-RSSI and Zappone *et al.* ANN-based schemes because it sets a residence time threshold, but it gives high priority to the cell that has the strongest signal power. Consequently, the A2T-KNN has superiority over the HO RTP method by 38.1%.

VI. CONCLUSION AND FUTURE WORK

In this paper, we study the cell selection problem of HetNets by using SDN and machine learning technologies. In this paper, an SDN/ML-based adaptive cell selection scheme called A2T-KNN is proposed. It is designed for two-tier HetNets and it can adapt to the characteristics of the network and the features of moving vehicles. The proposed A2T-KNN

TABLE 8. List of main abbreviations.

Abbreviation	Meaning
3GPP	3rd Generation Mobile Partnership Project
5G	Fifth Generation
A2T-KNN	Adaptive two-tier based on K-nearest neighbor
A3C	Asynchronous Advantage Actor Critic
ADA-CS	Adaptive Cell Selection
ADAM	Adaptive Moment
AN	Access Node
AS	Active Set
BSs	Base Stations
CA-MAB	Cell Association based on a Multi-Armed Bandit
CNN	Convolutional Neural Network
CoMP	Coordinated Multipoint
CRE	Cell Range Expansion
CRF	Conditional Random Field
CRF-CSP	CRF-Cell Selection Protocol
DDRL	Distributed Deep Reinforcement Learning
DQN	Deep Q-network
DS	Delay-Sensitive
DT	Delay-Tolerant
EE	Energy efficiency
FCS	Fast Cell Select
FF-ANN	Feed-Forward Artificial Neural Network
FFBP-ANN	Feed-Forward Back-Propagation Artificial Neural Network
G-mean	Geometric mean
HetNets	Heterogeneous Networks
HIT	Handover Interruption Time
HO	Handover
HO RTP	Handover based on Resident Time Prediction
iMACH	improved Movement-Aware CoMP Handover
IoT	Internet of Things
KMZ	Keyhole Markup Language
KNN	K-Nearest-Neighbor
KPIs	Key Performance Indicators
LAA	Licensed Assisted Access
MACH	Movement-Aware CoMP Handover
MAE	Mean Absolute Error
MDP	Markov Decision Process
MIMO	Multiple-Input and Multiple-Output
ML	Machine Learning
mmWave	millimeter Wave
NB	Naive Bayes
Ofcom	Office of Communications
PL	Path Loss
RANs	Radio Access Networks
ReLU	Rectified Linear Unit
RL	Reinforcement Learning
RLFs	Radio Link Failures
RMSE	Root Mean Square Error
RNN	Recurrent Neural Network
RRM	Radio Resource Management
RSS	Received Signal Strength
RSSI	Received Signal Strength Indicator
RSUs	Road Side Units
SDN	Software-Defined Networking
SINR	Signal-to-Interference-plus-Noise Ratio
TOPSIS	Technique for Order Preference by Similarity to Ideal Solution
UE	User Equipment
UK	United Kingdom
UMa-NLOS	Urban Macro-cell-Non-Line-Of-Sight
UMi-LOS	Urban Microcell-Line-Of-Sight

TABLE 9. List of main symbols.

Symbols	Description
$\mathbb{BS}s$	Set of all macro and small base stations
$\mathbb{BS}s_{macro}$	Set of macro BSs
$\mathbb{BS}s_{small}$	Set of small BSs
$\mathbb{BS}$	The serving BS
$\mathbb{V}$	Set of all vehicles
$\mathbb{A}$	Association matrix variables between vehicles and BSs
A_{ij}	Association variable between BS B_i and vehicle V_j
$\hat{S}$	Vehicle speed threshold
$\hat{L}$	Base stations load threshold
$\hat{RSSI}$	Received signal strength indicator threshold
LAT	Latitude coordinate of a vehicle
LON	Longitude coordinate of a vehicle
$AZIMUTH$	Angle between vehicle direction and the north
$KSPEED$	Speed of vehicle in km/h
ST_{ij}	Staying time of vehicle V_j within BS B_i
d_{ij}	Distance between BS B_i and vehicle V_j
Ω_{ij}	Angle between BS B_i and vehicle V_j
$RSSI_{ij}$	Received signal strength indicator value received by vehicle V_j from BS B_i
$\zeta(d)$	Path loss function over a distance
f_c	Carrier frequency
d'_{BP}	Break point distance
h_{Veh}	Height of vehicle
h_{BS}	Height of serving base station
h_{Eff}	Effective height
c	The speed of the light in vacuum
y	Target base stations
$\hat{y}$	Predicted base stations
N	Number of testing samples
Pr_f	Probability of handover failures
Pr_u	Probability of unnecessary handovers
R	Radius of a cell
v	Vehicle velocity
Th_f	Time threshold of handover failures
Th_u	Time threshold of unnecessary handovers
t_i	Handover delay to move into a serving cell
t_o	Handover delay to move out of a serving cell
$\overline{N}_f$	Average number of handover failures
$\overline{N}_u$	Average number of unnecessary handovers
$\overline{N}_{HO}$	Average number of handovers
C_{ij}	Channel capacity between BS B_i and vehicle V_j
γ_{ij}	Signal to interference plus noise ratio between BS B_i and vehicle V_j
p_{tx}	Transmission power of base station
g	The channel gain
N_0	Power spectral density of noise
BW	Channel bandwidth
η_{EE}	Energy efficiency of the system
SYN_{out}	Out-of-synchronization threshold
SYN_{in}	In-synchronization threshold
T_{RLF}	Timer of radio link failure

algorithm uses a KNN model that are trained based on realistic vehicle and BS information in the central area of London. Simulation results show that the trained model has a high prediction performance using the testing sample. In addition, our proposed A2T-KNN algorithm is superior to the traditional and HO RTP schemes in terms of the average number of HOs by 45.83% and 38.10%, respectively. Moreover, it enhances the average achievable DL throughput and

network energy efficiency achieved by vehicles by up to 17.18% and 16.86%, compared with the other methods. For future work, the A2T-KNN algorithm will be applied in other cities, such as the city of Riyadh, the capital of Saudi Arabia, based on the availability of macro and small BSs information. In addition, other machine learning algorithms can be applied and prediction performances can be compared. The cell selection issue in HetNets can be solved in subsequent studies based on reinforcement learning (RL) techniques, such as Q-learning and deep Q-networks (DQN). Licensed Assisted Access (LAA) deployment can be considered in our future work. It is a service that combines the use of licensed and unlicensed spectrum to enhance the achievable data rates and to improve the user response.

APPENDIX
LISTS OF ABBREVIATIONS AND SYMBOLS

The following table gives a list of abbreviations. Tables 8 and 9 give lists of the main abbreviations and symbols.

CONFLICTS OF INTEREST

The authors declare no conflict of interest.

REFERENCES

[1] M. Shammut, M. Cao, Y. Zhang, C. Papaix, Y. Liu, and X. Gao, "Banning diesel vehicles in London: Is 2040 too late?" *Energies*, vol. 12, no. 18, p. 3495, Sep. 2019.

[2] M. N. I. Sarker, M. N. Khatun, G. M. Alam, and M. S. Islam, "Big data driven smart city: Way to smart city governance," in *Proc. Int. Conf. Comput. Inf. Technol. (ICCIT)*, Sep. 2020, pp. 1–8.

[3] G. Contreras and F. Platania, "Economic and policy uncertainty in climate change mitigation: The London smart city case scenario," *Technol. Forecasting Social Change*, vol. 142, pp. 384–393, May 2019.

[4] I. Alablani and M. Alenazi, "EDTD-SC: An IoT sensor deployment strategy for smart cities," *Sensors*, vol. 20, no. 24, p. 7191, Dec. 2020.

[5] M. A. Nassar, L. Luxford, P. Cole, G. Oatley, and P. Koutsakis, "The current and future role of smart street furniture in smart cities," *IEEE Commun. Mag.*, vol. 57, no. 6, pp. 68–73, Jun. 2019.

[6] M. M. Alsulami and N. Akkari, "The role of 5G wireless networks in the Internet-of-Things (IoT)," in *Proc. 1st Int. Conf. Comput. Appl. Inf. Secur. (ICCAIS)*, Apr. 2018, pp. 1–8.

[7] I. Alablani and M. Alenazi, "Performance evaluation of sensor deployment strategies in WSNs towards IoT," in *Proc. IEEE/ACS 16th Int. Conf. Comput. Syst. Appl. (AICCSA)*, Nov. 2019, pp. 1–8.

[8] A. E. Azzaoui, S. K. Singh, Y. Pan, and J. H. Park, "Block5GIntell: Blockchain for AI-enabled 5G networks," *IEEE Access*, vol. 8, pp. 145918–145935, 2020.

[9] B. B. Kumar, L. Sharma, and S.-L. Wu, "Online distributed user association for heterogeneous radio access network," *Sensors*, vol. 19, no. 6, p. 1412, Mar. 2019.

[10] B. U. Kazi and G. A. Wainer, "Next generation wireless cellular networks: Ultra-dense multi-tier and multi-cell cooperation perspective," *Wireless Netw.*, vol. 25, no. 4, pp. 2041–2064, May 2019.

[11] S. P. Thiagarajah, M. Y. Alias, W.-N. Tan, and A. Mahmud, "Capacity optimised user association in planned small cell deployment for heterogeneous wireless networks," in *Proc. IEEE 5th Int. Symp. Telecommun. Technol. (ISTT)*, Nov. 2020, pp. 123–128.

[12] I. A. Alablani and M. A. Arafah, "An adaptive cell selection scheme for 5G heterogeneous ultra-dense networks," *IEEE Access*, vol. 9, pp. 64224–64240, 2021.

[13] H. Ramazanali, A. Mesodiakaki, A. Vinel, and C. Verikoukis, "Survey of user association in 5G HetNets," in *Proc. 8th IEEE Latin-Amer. Conf. Commun. (LATINCOM)*, Nov. 2016, pp. 1–6.

[14] I. A. Alablani and M. A. Arafah, "Enhancing 5G small cell selection: A neural network and IoV-based approach," *Sensors*, vol. 21, no. 19, p. 6361, Sep. 2021.

[15] S. Sonmez, I. Shayea, S. A. Khan, and A. Alhammadi, "Handover management for next-generation wireless networks: A brief overview," in *Proc. IEEE Microw. Theory Techn. Wireless Commun. (MTTW)*, Oct. 2020, pp. 35–40.

[16] L. C. Gimenez, P. H. Michaelsen, K. I. Pedersen, T. E. Kolding, and H. C. Nguyen, "Towards zero data interruption time with enhanced synchronous handover," in *Proc. IEEE 85th Veh. Technol. Conf. (VTC Spring)*, Jun. 2017, pp. 1–6.

[17] A. Gharsallah, F. Zarai, and M. Neji, "SDN/NFV-based handover management approach for ultradense 5G mobile networks," *Int. J. Commun. Syst.*, vol. 32, no. 17, p. e3831, Nov. 2019.

[18] K. Alexandris, N. Nikaein, R. Knopp, and C. Bonnet, "Analyzing X2 handover in LTE/LTE-A," in *Proc. 14th Int. Symp. Model. Optim. Mobile, Ad Hoc, Wireless Netw. (WiOpt)*, May 2016, pp. 1–7.

[19] K. Pieszko, J. Hiczkiewicz, P. Budzianowski, J. Budzianowski, J. Rzeźniczak, K. Pieszko, and P. Burchardt, "Predicting long-term mortality after acute coronary syndrome using machine learning techniques and hematological markers," *Disease Markers*, vol. 2019, pp. 1–9, Jan. 2019.

[20] O. A. Alimi, K. Ouahada, and A. M. Abu-Mahfouz, "A review of machine learning approaches to power system security and stability," *IEEE Access*, vol. 8, pp. 113512–113531, 2020.

[21] M. Alsaeedi, M. M. Mohamad, and A. A. Al-Roubaiey, "Toward adaptive and scalable OpenFlow-SDN flow control: A survey," *IEEE Access*, vol. 7, pp. 107346–107379, 2019.

[22] A. Papazafeiropoulos, P. Kourtessis, M. Di Renzo, J. M. Senior, and S. Chatzinotas, "SDN-enabled MIMO heterogeneous cooperative networks with flexible cell association," *IEEE Trans. Wireless Commun.*, vol. 18, no. 4, pp. 2037–2050, Apr. 2019.

[23] E. Ganesan, I.-S. Hwang, A. T. Liem, and M. S. Ab-Rahman, "SDN-enabled FiWi-IoT smart environment network traffic classification using supervised ML models," *Photonics*, vol. 8, no. 6, p. 201, Jun. 2021.

[24] Y. M. Waheidi, M. Jubran, and M. Hussein, "User driven multiclass cell association in 5G HetNets for mobile & IoT devices," *IEEE Access*, vol. 7, pp. 82991–83000, 2019.

[25] Y. Yang, J. Xu, G. Shi, and C.-X. Wang, *5G Wireless Systems*. Berlin, Germany: Springer, 2018.

[26] R. Abdullah and Z. Zukarnain, "Enhanced handover decision algorithm in heterogeneous wireless network," *Sensors*, vol. 17, no. 7, p. 1626, Jul. 2017.

[27] P. Fan, J. Zhao, and C.-L. I, "5G high mobility wireless communications: Challenges and solutions," *China Commun.*, vol. 13, no. 2, pp. 1–13, 2016.

[28] R. Arshad, H. Elsawy, S. Sorour, T. Y. Al-Naffouri, and M.-S. Alouini, "Handover management in 5G and beyond: A topology aware skipping approach," *IEEE Access*, vol. 4, pp. 9073–9081, 2016.

[29] F. B. Tesema, A. Awada, I. Viering, M. Simsek, and G. P. Fettweis, "Fast cell select for mobility robustness in intra-frequency 5G ultra dense networks," in *Proc. IEEE 27th Annu. Int. Symp. Pers., Indoor, Mobile Radio Commun. (PIMRC)*, Sep. 2016, pp. 1–7.

[30] A. S. Cacciapuoti, "Mobility-aware user association for 5G mmWave networks," *IEEE Access*, vol. 5, pp. 21497–21507, 2017.

[31] D. S. Wickramasuriya, C. A. Perumalla, K. Davaslioglu, and R. D. Gitlin, "Base station prediction and proactive mobility management in virtual cells using recurrent neural networks," in *Proc. IEEE 18th Wireless Microw. Technol. Conf. (WAMICON)*, Apr. 2017, pp. 1–6.

[32] A. Kishida, Y. Morihiro, T. Asai, and Y. Okumura, "Cell selection scheme for handover reduction based on moving direction and velocity of UEs for 5G multi-layered radio access networks," in *Proc. Int. Conf. Inf. Netw. (ICOIN)*, Jan. 2018, pp. 362–367.

[33] S. Q. Zhang, F. Xue, N. A. Himayat, S. Talwar, and H. T. Kung, "A machine learning assisted cell selection method for drones in cellular networks," in *Proc. IEEE 19th Int. Workshop Signal Process. Adv. Wireless Commun. (SPAWC)*, Jun. 2018, pp. 1–5.

[34] A. Zappone, L. Sanguinetti, and M. Debbah, "User association and load balancing for massive MIMO through deep learning," in *Proc. 52nd Asilomar Conf. Signals, Syst., Comput.*, Oct. 2018, pp. 1262–1266.

[35] D. P. Kingma and J. Ba, "Adam: A method for stochastic optimization," in *Proc. Int. Conf. Learn. Represent.*, 2015, pp. 1–15.

[36] M. Elkourdi, A. Mazin, and R. D. Gitlin, "Towards low latency in 5G HetNets: A Bayesian cell selection/user association approach," in *Proc. IEEE 5G World Forum (5GWF)*, Jul. 2018, pp. 268–272.

[37] H. Khan, A. Elgabli, S. Samarakoon, M. Bennis, and C. S. Hong, "Reinforcement learning-based vehicle-cell association algorithm for highly mobile millimeter wave communication," *IEEE Trans. Cognit. Commun. Netw.*, vol. 5, no. 4, pp. 1073–1085, Dec. 2019.
[38] Q. Liu, C. F. Kwong, S. Zhang, L. Li, and J. Wang, "A fuzzy-clustering based approach for MADM handover in 5G ultra-dense networks," *Wireless Netw.*, pp. 1–14, Sep. 2019.
[39] Y. M. Waheidi, M. Jubran, and M. Hussein, "User driven multiclass cell association in 5G HetNets for mobile IoT devices," *IEEE Access*, vol. 7, pp. 82991–83000, 2019.
[40] Y. Zhang, L. Xiong, and J. Yu, "Deep learning based user association in heterogeneous wireless networks," *IEEE Access*, vol. 8, pp. 197439–197447, 2020.
[41] W. Sun, L. Wang, J. Liu, N. Kato, and Y. Zhang, "Movement aware CoMP handover in heterogeneous ultra-dense networks," *IEEE Trans. Commun.*, vol. 69, no. 1, pp. 340–352, Jan. 2021.
[42] Z. Qin, W. Feng, Z. Yue, and H. Tian, "A handover management strategy using residence time prediction in 5G ultra-dense networks," in *Signal and Information Processing, Networking and Computers*. Singapore: Springer, 2021, pp. 808–816.
[43] I. Yaqoob, I. Ahmad, E. Ahmed, A. Gani, M. Imran, and N. Guizani, "Overcoming the key challenges to establishing vehicular communication: Is SDN the answer?" *IEEE Commun. Mag.*, vol. 55, no. 7, pp. 128–134, Jul. 2017.
[44] W. Zhuang, Q. Ye, F. Lyu, N. Cheng, and J. Ren, "SDN/NFV-empowered future IoV with enhanced communication, computing, and caching," *Proc. IEEE*, vol. 108, no. 2, pp. 274–291, Feb. 2020.
[45] O. Boswarva. (Feb. 2017). *Sitefinder Mobile Phone Base Station Database*. [Online]. Available: https://datashare.ed.ac.U.K./handle/10283/2626
[46] P. Romero-Fresco, "Accessing communication: The quality of live subtitles in the U.K.," *Lang. Commun.*, vol. 49, pp. 56–69, Jul. 2016.
[47] "Technical specification group radio access network; Study on channel model for frequencies from 0.5 to 100 GHz," 3GPP, Tech. Rep. 38.901, V16.1.0 (Release 16), 2019.
[48] K. Zia, N. Javed, M. N. Sial, S. Ahmed, A. A. Pirzada, and F. Pervez, "A distributed multi-agent RL-based autonomous spectrum allocation scheme in D2D enabled multi-tier HetNets," *IEEE Access*, vol. 7, pp. 6733–6745, 2019.
[49] C. K. Sung, S. Li, M. Hedley, N. Nikolic, and W. Ni, "Skew log-normal channel model for indoor cooperative localization," in *Proc. IEEE 28th Annu. Int. Symp. Pers., Indoor, Mobile Radio Commun. (PIMRC)*, Oct. 2017, pp. 1–5.
[50] R. Wang, X. Liang, X. Zhu, and Y. Xie, "A feasibility of respiration prediction based on deep Bi-LSTM for real-time tumor tracking," *IEEE Access*, vol. 6, pp. 51262–51268, 2018.
[51] W. Wu, "Weakly supervised learning by a confusion matrix of contexts," in *Proc. Pacific-Asia Conf. Knowl. Discovery Data Mining*. Cham, Switzerland: Springer, 2019, pp. 59–64.
[52] S. Ruskaa, W. Hämäläinen, S. Kajava, M. Mughal, P. Matilainen, and J. Mononen, "Evaluation of the confusion matrix method in the validation of an automated system for measuring feeding behaviour of cattle," *Behav. Processes*, vol. 148, pp. 56–62, Mar. 2018.
[53] C. Wu, X. Cai, J. Sheng, Z. Tang, B. Ai, and Y. Wang, "Parameter adaptation and situation awareness of LTE-R handover for high-speed railway communication," *IEEE Trans. Intell. Transp. Syst.*, early access, Oct. 6, 2020, doi: 10.1109/TITS.2020.3026195.
[54] R. Ahmad, E. A. Sundararajan, N. E. Othman, and M. Ismail, "Handover in LTE-advanced wireless networks: State of art and survey of decision algorithm," *Telecommun. Syst.*, vol. 66, no. 3, pp. 533–558, 2017.
[55] L. Tuyisenge, M. Ayaida, S. Tohme, and L.-E. Afilal, "A mobile internal vertical handover mechanism for distributed mobility management in VANETs," *Veh. Commun.*, vol. 26, Dec. 2020, Art. no. 100277.
[56] S. Biswas, A. Gupta, and S. Chakraborty, "Load-balanced user associations in dense LTE networks," *Comput. Netw.*, vol. 189, Apr. 2021, Art. no. 107928.
[57] I. A. Alablani and M. A. Arafah, "Applying a dwell time-based 5G V2X cell selection strategy in the city of Los Angeles, California," *IEEE Access*, vol. 9, pp. 153909–153925, 2021.
[58] R. Hussain, S. A. Malik, S. Abrar, R. A. Riaz, H. Ahmed, and S. A. Khan, "Vertical handover necessity estimation based on a new dwell time prediction model for minimizing unnecessary handovers to a WLAN cell," *Wireless Pers. Commun.*, vol. 71, no. 2, pp. 1217–1230, Jul. 2013.
[59] I. Allal, B. Mongazon-Cazavet, K. Al Agha, S.-M. Senouci, and Y. Gourhant, "A green small cells deployment in 5G—Switch on/off via IoT networks & energy efficient mesh backhauling," in *Proc. IFIP Netw. Conf. (IFIP Netw.) Workshops*, 2017, pp. 1–2.
[60] J. F. Valenzuela-Valdés, N. Palomares, J. C. González-Macías, A. Valenzuela-Valdés, P. Padilla, and F. Luna-Valero, "On the ultra-dense small cell deployment for 5G networks," in *Proc. IEEE 5G World Forum (5GWF)*, Jul. 2018, pp. 369–372.
[61] A. Dataesatu, P. Boonsrimuang, K. Mori, and P. Boonsrimuang, "Energy efficiency enhancement in 5G heterogeneous cellular networks using system throughput based sleep control scheme," in *Proc. 22nd Int. Conf. Adv. Commun. Technol. (ICACT)*, Feb. 2020, pp. 549–553.
[62] Z.-H. Huang, Y.-L. Hsu, P.-K. Chang, and M.-J. Tsai, "Efficient handover algorithm in 5G networks using deep learning," in *Proc. IEEE Global Commun. Conf. (GLOBECOM)*, Dec. 2020, pp. 1–6.
[63] X. Ba and Y. Wang, "Load-aware cell select scheme for multi-connectivity in intra-frequency 5G ultra dense network," *IEEE Commun. Lett.*, vol. 23, no. 2, pp. 354–357, 2019.
[64] M. Polese, M. Giordani, M. Mezzavilla, S. Rangan, and M. Zorzi, "Improved handover through dual connectivity in 5G mmWave mobile networks," *IEEE J. Sel. Areas Commun.*, vol. 35, no. 9, pp. 2069–2084, Sep. 2017.
[65] H.-S. Park, Y. Lee, T.-J. Kim, B.-C. Kim, and J.-Y. Lee, "Handover mechanism in NR for ultra-reliable low-latency communications," *IEEE Netw.*, vol. 32, no. 2, pp. 41–47, Mar./Apr. 2018.
[66] A. Alhammadi, M. Roslee, M. Y. Alias, I. Shayea, and S. Alraih, "Dynamic handover control parameters for LTE-A/5G mobile communications," in *Proc. Adv. Wireless Opt. Commun. (RTUWO)*, Nov. 2018, pp. 39–44.

IBTIHAL AHMED ALABLANI received the B.S. degree in computer science from Princess Nourah Bint Abdulrahman University, in 2008, and the M.S. degree in computer engineering from King Saud University, in 2013, where she is currently pursuing the Ph.D. degree with the Computer Engineering Department. Since 2008, she has been working at Technical and Vocational Training Corporation (TVTC)/Technical College as a Faculty Member. Her research interests include wireless sensor networks, 5G heterogeneous networks, smart cities, and machine learning. She was awarded a Certificate of Excellence from the Saudi Ministry of Education as one of the top students in Saudi Arabia at high school, in 2004.

MOHAMMED AMER ARAFAH received the B.S. degree from King Saud University and the M.S. and Ph.D. degrees from the University of Southern California, USA. He is currently an Associate Professor in computer engineering. His research interests include computer network modeling and simulation, wireless sensor networks, cooperative relay networks, fault tolerance, 5G heterogeneous networks, and high-speed networks.